AN OIM STUDY ON THE VARIANT SELECTION PHENOMENNON IN AN Fe-30Ni ALLOY

ИССЛЕДОВАНИЕ ЯВЛЕНИЙ ВЫБОРА ВАРИАНТОВ ПРЕВРАЩЕНИЯ В СПЛАВЕ FeNi30 С ПРИМЕНЕНИЕМ МЕТОДА ОРИЕНТАЦИОННОГО АНАЛИЗА МИКРОСТРУКТУРЫ.

Dr. Eng. Petrov R., Prof. Dr. Ir. Kestens L. and Prof. Dr. Ir. Houbaert Y.

Gent University-Belgium

e-mail: Roumen.Petrov@UGent.be

***Abstract**: A variant selection phenomenon during the phase transformation in an Fe-30% Ni alloy was studied by means of the EBSD technique. The samples were slowly cooled to room temperature at a rate of 1°C/min after reheating to 1100°C, or warm rolling at ~250°C after air cooling, which is 20°C below the so called M^{σ}_{S} temperature of the alloy. The crystallographic orientations of parent austenite and product martensite phases were determined on the basis of local measurements. The measured product textures were compared with the modeled ones, which were obtained by applying the Bain, Kurdjumov–Sachs and Nishiyama-Wassermann transformation laws on the local austenite grains. It was shown that the presence of a deformation substructure is not an essential prerequisite for the occurrence of variant selection. The data reveal that a variant selection mechanism is active also in not deformed samples, containing a fully recrystallized parent matrix.*

Keywords: martensite transformation, variant selection, EBSD

1. Introduction

As it is well known a specific crystallographic relation connects the parent and product orientations during the diffusionless γ(FCC) to α_M (BCC) phase transformation. The most frequently used are orientation correspondences were proposed by Kurdjumov – Sachs (K-S), Nishiyama – Wassermann (N-W), Greninger-Troiano and Bain. Usually these orientation relationships are described by the planes and directions from the parent and product phase that remain parallel to each during the transformation, but very often the axis–angle representation is used as well (Table1).

Table 1. Main crystallographic orientation relationships in BCC-FCC transformation

	Corresponding Directions	Corresponding Planes	Orientation relation	Number of Variants
Bain	[110]γ//[010]α	(001)γ//(001)α	<100>45°	3
K-S	[101]γ//[111]α	(111)γ//(110)α	<112> 90°	24
N-W	[211]γ//[011]α	(111)γ//(110)α	<362>95,3°	12

As it can be seen from Table 1 each crystallographic orientation relationship predicts different numbers of product orientations originating from a single crystallographic orientation of the parent phase. It means that theoretically a single FCC orientation after transformation to BCC has to give rise to 24 K-S, 12 N-W or 3 Bain variants depending on the chemical composition of the alloy. In reality only few of the theoretically predicted variants appear and this phenomenon is known as ***variant selection***.

The variant selection is clearly manifested during the martensitic transformation which is strongly influenced by the stress and strain state in the transforming volume. As a consequence, specific orientations with respect to the applied stress will develop crystallographic variants and grow at the expense of others with a less favorable orientation. This phenomenon was described and discussed in a lot of studies [1-4] from different viewpoints.

Humbert *et al* [2] test the assumptions that the average selected variants are those which induce the maximal deformation perpendicular to the sheet, or the assumption that the selected variants are these which produce the minimal deformation in the plane of the sheet. They find experimental evidences for the second hypothesis. In a later work *Liu and Bunge*[3] studied the martensite transformation of Fe-30%Ni with a strong cube texture, applying the N-W orientation relation. They found that a plastic deformation prior to the transformation leads to selection rules for the orientation as well as for the habit plane variants and associate the phenomenon with the different activity of the slip planes and slip directions during the foregoing deformation. Recently *Wittridge and Jonas*[4] tested a dislocation reaction model for variant selection under the condition of torsion (simple shear). The model is based on a correspondence between the K-S transformation products and the 24 possible Bishop and Hill slip systems, and was proposed earlier by *Sum and Jonas* [5] for three simple strain paths, namely plane strain rolling [5], axisymmetric compression[6] and axisymmetric extension [7]. They found an excellent prediction for the transformation textures resulting from the preceding deformation.

In all of these models the martensite transformation develops in a previously deformed matrix, which is characterized by a given distribution of defects (dislocations, stacking faults) and their mobility that favor the nucleation of the specific variants. In the studies mentioned above the bulk texture was measured by means of the XRD method or neutron diffraction in order to approve the validity of the models. Even when the martensite transformation develops in non-stressed or strained conditions not all of the theoretically predicted variants are presented in the martensite phase. The textures calculated by means of the orientations relation predicted by K-S and N-W in some instances fit well to the experimental data but more often only a part of theoretically calculated variants are really presented in the experimental texture. Undoubtedly this is an indication for the variant selection during the transformation when the external stress (strain) is not applied, which cannot readily be explained by the above models.

Recently new observation techniques like EBSD allow easy, fast and precise local orientation measurements in the two phase materials, which gives possibilities for a more detailed study of the orientation selection phenomenon.

The goal of the present work is to study the orientation selection phenomenon during a martensitic transformation and more specifically to study the effect of the deformation substructure, which was introduced by applying a rolling treatment prior to the martensitic transformation. The orientation relation between parent and product components will be monitored locally by executing local orientation determinations employing the well-known EBSD- technique. Although extra low carbon steel is the material of interest it was chosen nevertheless, to carry out the present work on an Fe-Ni alloy, because in this material the parent austenite phase is stable at much lower temperatures, as compared to the conventional low-carbon steels. Hence, an Fe-Ni alloy is much more suitable to study par-

tially transformed structures at room temperature in which both the parent austenite and product martensite co-exist.

2. Experimental

An Fe –Ni alloy with a composition shown in table 2 was melted under Ar in a quantity of 100 kg; cut in pieces with size 250 x120 x 25 mm; reheated to 1250°C and hot rolled to a final thickness of 4 mm. The final rolling temperature was 750 °C. The value of the critical temperatures was determined by dilatometry tests on the as cast and hot rolled specimens with a reheating rate of 5°C/s and different cooling rates varying form 5°C/s to ~700°C/s (quenching in He gas flow).

A part of the as hot rolled samples were reheated again to 1000°C and after isothermal soaking of 1 hour were cooled down to 100°C with a cooling rate of 1°C/min. The goal of this treatment was to create conditions for martensite transformation in recrystallized austenite avoiding even the influence of the thermal stresses on the transformation.

Table 2. Chemical composition of the alloy, in mass %.

Ni	*C*	*Si*	*Mn*	*P*	*S*	*Al*
27.9	0.019	0.009	0.2	0.016	0.013	0.077

Other samples were reheated to 1000 °C and after 1 hour soaking were air cooled to 250 °C and rolled in one pass of 37% reduction (Fig.1). By means of this thermo-mechanical treatment we have tried to provoke a rise only of strain induced martensite in the recrystallized austenite matrix (Fig.1.(a)) Actually, before the transformation the austenite matrix will also accumulate a part of the plastic deformation.

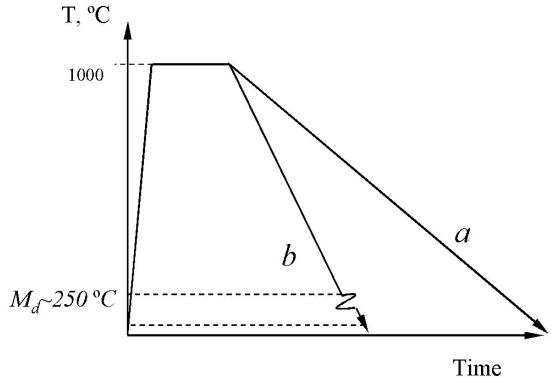

Fig.1: Schematic representation of the thermo-mechanical treatment of the samples. (a) cooling to RT at 1°C/min; (b) air cooling to 250°C and rolled in one pass with 37% reduction.

Specimens of size 15 x 5 x 4 mm were cut from the as processed sheet parallel to the rolling direction (RD). Samples for observation with Light Optical Microscopy(LOM) were prepared following the standard grinding and polishing procedure described elsewhere [8]

The micro texture analysis was carried out by employing an Orientation Imaging Microscopy (OIM) attachment installed on a FEI XL30 ESEM microscope with an LaB_6 filament. The OIM scans were collected in a plane perpendicular to the transverse direction (TD). The electron backscattering diffraction (EBSD) patterns were acquired and analyzed by means of the TSL® software. The OIM data were further post-processed with the texture software developed by Van Houtte [9] and the orientation distribution function (ODFs) for the austenite and martensite phase were calculated. Kurdjumov–Sachs, Nishiama–Wasermann and Bain orientation relationships were applied to the experimentally measured data for the austenite phase by means of the analytical procedure and supporting software that were develop for the purpose of this study. The ODFs obtained by this simulation were compared and analyzed together with the ODFs calculated on the basis of the measured martensite orientations. More than 40 individual grains (orientations) were examined but only few representative data are displayed in this work.

3. Results and discussion

The microstructures of the material after 37% rolling reduction at 250 °C and after slow cooling (of 1°C/min) are shown in Fig. 2a in Fig.2 b, respectively. The amount of austenite phase is 50%, for the samples warm rolled at ~250°C (above the Ms temperature according to regime (b) Fig. 1) and 40 % for samples cooled with 1°C/min (regime (a) Fig. 1). In both groups of samples the amount of parents FCC phase is enough to be clearly identified and the grain boundary of the parent austenite grains are easily detectable. This allows identifying in a proper way the parent grain of each group of product BCC orientations. The EBSD study allows a more accurate identification of the exact crystallographic orientation of the individual parent (FCC) and product (BCC) phases.

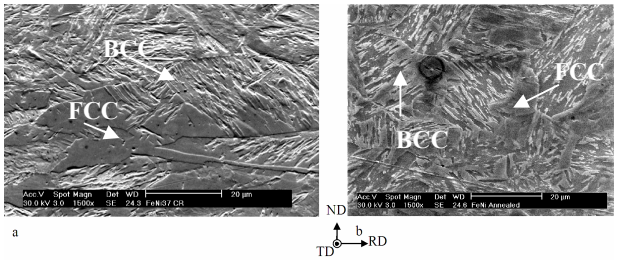

Fig.2 Microstructure of (a) sample 37% rolled at 250° and (b) cooled to room temperature at 1C/min from 1000°C;

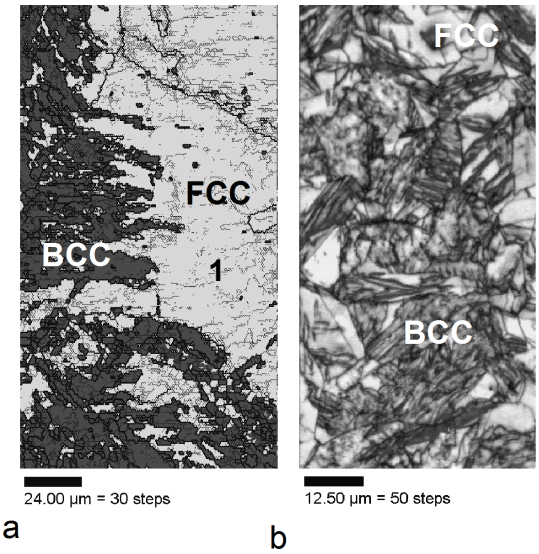

Fig. 3: Gray scale phase map displaying BCC and FCC phases with grain boundaries (GB) in (a) annealed at 1000°C and rolled 37% at 250°C sample and (b) Image quality map of sample annealed at 1000°C and slowly cooled.

Fig. 3a display the phase distribution map obtained by an OIM scan of the sample reheated to 1000°C and rolled in one pass at 250°C with a reduction of 37%. The FCC phase (white) accumulates part of the deformation and its substructure is changed. An increased amount of low angle grain boundaries (thin black lines) is clearly observed inside the FCC phase. The high angle grain boundaries (misorientation between 15 and 180°) are displayed with thick black lines which delineate the individual FCC grains. The FCC phase in slowly cooled samples (Fig.3b, white zones) does not display a subgrain structure i.e. one can suppose that the γ-α transformation develops in a virtually defects free γ matrix. Hence, the influence of the pre-existing defects on the martensitic variants can be excluded in this case. The individual parent and product orientations were selected on the basis of the colour code orientation maps in which

each crystallographic orientation appears in a unique colour. This approach gives several important possibilities: *(i)* to determine the exact orientation of the parent FCC grain; *(ii)* to post-process the *orientation of the parent phase* and to calculate the possible *product orientations* by means of various transformation models (K-S, N-W and Bain), *(iii)* to measure directly the orientation of the product phase originating from only one parent and *(iv)* to use the orientation data for calculation of the *misorientation* between parent and product phase. An example for such a partition procedure is displayed in Fig.4.

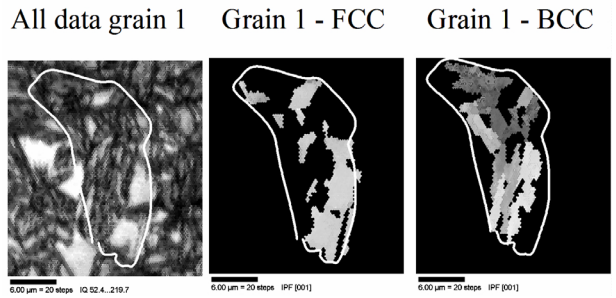

Fig. 4: (a) Combined Image Quality and Phase map; (b) Orientation map of FCC phase; (c) orientation map of BCC phase. The differences in the grey levels correspond to different orientations.

Fig.5 displays the orientations that are representative for the group of the samples *slowly cooled* to room temperature. The parent austenite phase has an orientation given by Euler angles φ1= 90 ±5°; Φ=43±5° and φ2=323±5° that corresponds to the {223}⟨334⟩ texture component.

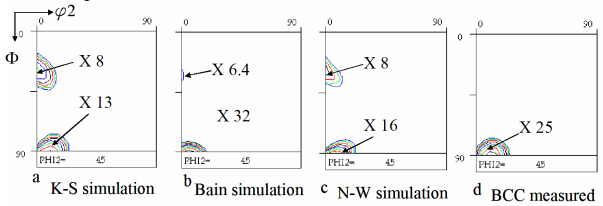

Fig.5: ODF of the martensite phase in a φ_2=45° section (a) K-S simulation; (b) Bain simulation; (c) N-W simulation; (d) measured martensite texture.

only one crystallographic variant is observed. Therefore, even in the case of slow cooling when the parent phase matrix is free of stresses and without any developed substructure, the effect of the variant selection is clearly observed.

A representative grain for the sample that was rolled prior to transformation are analysed in Fig. 6.The parent austenite grain (grain1 Fig.3a) has a well developed deformation substructure and displays crystallographic orientations with a spread of more then 10° around φ1=21°; Φ=23° and φ2=48° (the {113}⟨361⟩ texture component). The predicted transformation products together with the measured ones are shown in fig.6. For the representation of the BCC textures by means of ODFs it is usually sufficient to display only the φ2=45° section of the Euler space because the most important BCC texture components are presented in this section. In this case the model predictions do not display any texture components in the φ2=45° section, so, the φ1=145°and φ1=205° sections in which the predicted product texture components appear with the maximum intensity will be discussed.

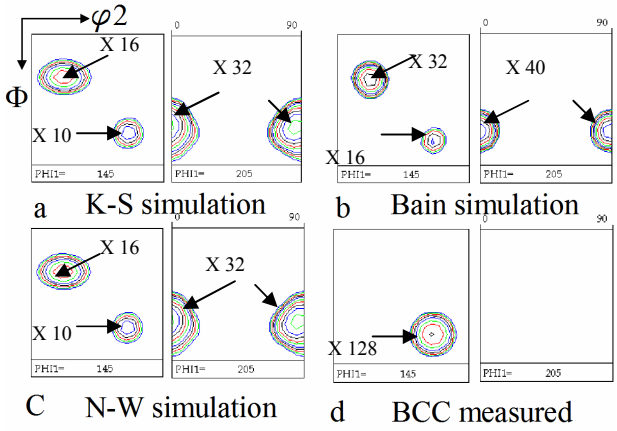

Fig.6: ODF of the martensite phase in a φ_1=145° and φ_1=205°sections of Euler space. (a) K-S simulation; (b) Bain simulation; (c) N-W simulation; (d) measured martensite texture.

In this case all three models predict the same product BCC orientations with only a difference in the texture intensity which is a consequence of the different number of variants predicted by the models (fig.6a-c). The measured ODF (fig.6d) displays that the parent

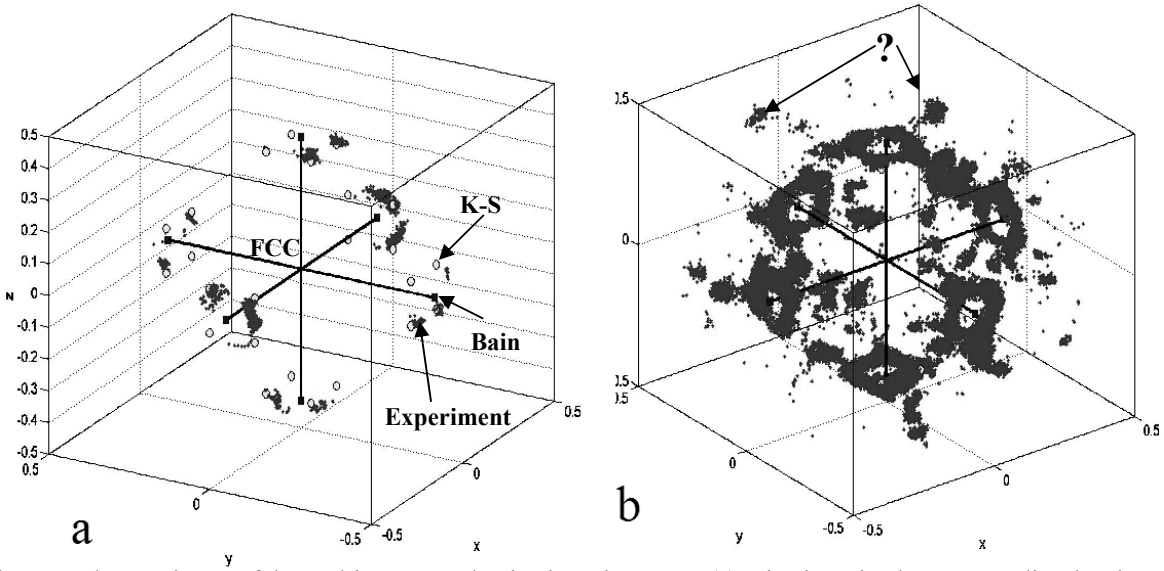

Fig.7: Fundamental zone of the Rodrigues –Frank misorientation space. (a) Misorientation between predicted and measured transformation products originating from a single austenite grain; (b) Same for 9 individual FCC orientations. Bain–black squares, K-S-white dots, measured misorientation – small grey dots. Slow cooled sample.

All three transformation model predict the appearance of *two* product BCC variants with different intensity. In the real measurement

phase transforms to a single product crystallographic variant. The rest of the predicted variants are not presented in the experimentally measured ODF. Therefore, the material transformed under stress (strain) displays clear variant selection as it was expected.

In order to obtain statistically reliable results, the experimental data were reprocessed and plotted in a three-dimensional misorientation space known as Rorigues-Frank space. In this space one can evaluate the deviation from the experimentally observed misorientations (between product and parent grains) and the reference correspondences according to the various models (Bain and K-S in this case), represented by misorientation axes and misorientation angles. Each axis-angle pair $\mathbf{d}\omega$ is represented in this space by the Rorigues – Frank vector, defined as $\mathbf{R}=\mathbf{d}.\mathrm{tg}(\omega/2)$. In this equation **R** is Rodrigues-Frank vector, **d** is the misorientation axis with coordinates $\mathbf{(d_1, d_2, d_3)}$ and ω is the minimum misorientation angle. For example for K-S orientation relationship **d** is (0.178, 0.178, 0.968) and ω is 42.85°, whereas for the Bain orientation relation the corresponding values are $\mathbf{d}\langle 001\rangle$, and $\omega = 45°$. Each point in Fig.7a displays the misorientation between the calculated and measured transformation products originating from a single FCC orientation (cross point in the middle). It is obvious that: *(i)* the experimentally measured products are grouped only around calculated K-S (24 white points) orientations but not around the predicted Bain (6 black squares) variants; (ii) not all of the predicted K-S variants are presented – i.e. the variant selection phenomenon exists even when the transformation develops in a virtually "defects-free" matrix of the parent phase. This conclusion is confirmed by the study of a large number of individual grains. Fig. 7b displays the misorientations between predicted and measured BCC transformation products originating from 9 individual FCC orientations in the slowly cooled samples. It can be clearly seen that the calculated Bain orientation relationships are not among the experimentally measured ones, whereas most of the experimental results coincide with the calculated the K-S orientation.

It is important to be mentioned that additional crystallographic variants ($\{114\}\langle 221\rangle$) which were not predicted by any of the explored transformation models were observed in the experimental data for samples with or without a pre-transformation strain (Fig.7b the misorientations with a question mark). These not-predicted orientations are observed also in the measured ODFs of BCC phase (Fig.8 a) and are more obviously presented in the samples deformed prior to transformations.

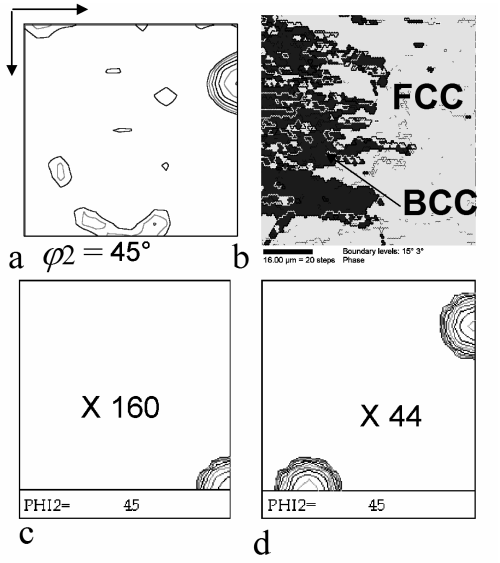

Fig.8: (a) ODF of product phase measured in strained prior to transformation sample (Fig.3, zone 2); (b)Phase map with $\langle 111\rangle \pm 60°$ axis–angle grain boundaries (in white), situated mainly in BCC phase; (c) ODF of Goss orientation (simulation); (d) ODF of the Goss orientation after rotation ±60° about $\langle 111\rangle$ axis.

Therefore, it could be suggested that they are associated to additional deformation in the product BCC phase. Taking into account that in this sample the martensite phase nucleates and grows under strain one can suppose that an additional BCC twinning component is observed in the ODF of Fig 8a.

If this is a twinning component it can be only a deformation twinning component of the BCC orientation and it can emerge only from an already existing orientation in the BCC phase (i.e. predicted by one of the transformation models). It is well known that the mechanical twinning in BCC has a K_1 $\{112\}$ twinning plane and a η_1 $\langle 111\rangle$ twinning direction. The BCC orientation after mechanical twinning can be presented as a rotation of ± 60° about a common $\langle 111\rangle$ axis. Using this approach a simulation of the mechanical twinning of different initial BCC orientations was carried out and the results are shown in Fig. 8c,d. It was found that the measured $\{114\}\langle 221\rangle$ BCC component can emerge from a BCC Goss component which is predicted by all of the models [8]. Additional independent approval of this assumption was found by means of delineation of the $(\pm 60°\langle 111\rangle)$ axis-angle grain boundaries in the phase map in TSL software (Fig.8b). The $\pm 60°\langle 111\rangle$ axis-angle grain boundaries with a spread of 10° are printed in white in Fig.8b. They are situated exclusively in the BCC zones, and almost do no appear in the parent FCC phase, which supports the assumption of their origin.

4. Conclusions

The variant selection phenomenon in an Fe –30%Ni was studied by means of EBSD technique in two different conditions of the parent matrix prior to transformation: either annealed or deformed. The misorientations between predicted and measured orientations are calculated and the results are presented in the Rodrigues-Frank space. The results can be summarized as follows:

- A strong variant selection phenomenon was observed in the strained samples (as it was expected) but also in the non-strained samples (as it was not expected).
- Variants were observed in the product phase of both groups of samples that were not predicted by the existing models. Their origin is associated with additional twining of the product components in the BCC phase.
- K-S orientation relationship gives the better description of the orientation relations during the transformation in comparison to the Bain model.
- Representation of the results of individual EBSD measurements in the Rodrigues-Frank space is an effective and powerful way for the quantitative study of variant selection phenomenon.

5. Acknowledgments

The authors gratefully acknowledge the financial support for this work from the Nederland Institute for Metals Research (NIMR), under contract MC 5.01109.

6. References

[1] R.K. Ray, J.J. Jonas: *International Materials Reviews*, **35** (1990), 30.

[2] M. Humbert, F. Wagner , W.P. Liu, C. Esling, H.J. Bunge: Proc. of 8th Int. Conf. on Textures of Materials, Warrendale , PA, AIME, 1988, p.743.

[3] W.P. Liu,H.J. Bunge: *Materials Letters*, **10**, (1991), 343.

[4] N.J. Wittridge, J.J. Jonas.: *Acta mater*, **48, (**2000), 2737.

[5] M.Sum, J.J. Jonas: *Textures Microstructures*, **31**, (1999), 187.

[6] M. Sum, J.J. Jonas, J.H. Root: In Proc. of 12th Int. Conf. On Texture of Materials (ICOTOM 12), Montreal, National Research Council of Canada, (1999), 761.

[7] N.J. Wittridge, J.J.Jonas, J.H. Root: In Proc. of 12th Int. Conf. On Texture of Materials (ICOTOM 12), National Research Council of Canada, (1999), 1089.

[8] L.Kestens, R.Petrov, Y. Houbaert: *ISIJ International*, Vol. 43, (2003) No.9, 1444-1452.

[9] P. Van Houte: User manual, MTM-FHM Software, Ver., 2 ed. By MTM-KULeuven, (1995), private communication.